



Functionalized Halloysite Nanotubes and Graphene Oxide Nanosheets Fillers Incorporated in UF Membranes for Oil/Water Separation

M. Amid, N. Nabian*, M. Delavar

Department of Chemical Engineering, University of Science and Technology of Mazandaran, Behshahr, Iran

PAPER INFO

Paper history:

Received 10 March 2023

Received in revised form 11 April 2023

Accepted 18 April 2023

Keywords:

Dual Nanofillers

Graphene Oxide Nanomaterials

SDS-functionalized Halloysite Nanotubes

Polycarbonate Polymer

ABSTRACT

Novel ultrafiltration mixed matrix membranes combined by dual nanofillers Graphene Oxide + Functionalized Halloysite Nanotubes (GO/FHNTs) were prepared. In this work, we improved the performance and properties of polycarbonate-based membranes for oil/water separation applications. The morphology and other properties of the fabricated membranes were characterized by different analytical method including Field Emission Scanning Electron Microscope (FESEM), Fourier-transform infrared spectroscopy (FTIR), contact angle goniometer, and mechanical strength apparatus. The obtained results confirmed that addition of GO/FHNTs had a positive effect on hydrophilicity and tensile strength. Also, the water permeation of the optimum GO0.25-FHNT0.75 membrane was about 2.5 times more than pure polycarbonate. Overall results showed that all membranes reached 100% oil separation efficiency at various ultrafiltration times. Furthermore, the optimum membrane showed a flux recovery ratio of more than 90% where the permeate fluxes of feed solutions with 100 ppm and 200 ppm olive oil concentrations were reduced to only about 5.5% and 6% after three regeneration cycles, respectively.

doi: 10.5829/ije.2023.36.07a.01

1. INTRODUCTION

Today, the separation of oil from water has received a lot of attention. One of the main reasons in this regard is the increasing demand for purified and clean water. Oily wastewater is the product of various industries such as steel, food industry and pharmacy. These wastewaters can also enter to open water during oil exploration and transportation [1]. Nowadays, the scarcity of clean water has become a serious problem, due to the rapid increase in population and industrial activities [2, 3]. The most common methods of purifying oily wastewater can be named as centrifugal systems, cyclones, electrostatic precipitation, and membrane filtration [4-6]. Among the various techniques, membrane filtration is a more effective and efficient one for separating oil from wastewaters, especially oil emulsions. The advantages of membrane separation are high selectivity, low maintenance cost, low required space, high efficiency, and no need for chemical additives [7-9]. Hence,

different studies have been done by researchers in which membrane separation processes were used for the decontamination of oily pollutants [10-13]. Among these applied pressure gradient membrane processes, ultrafiltration systems are of great importance owing to their lower required pressures compared to others [14, 15]. Nowadays, mixed matrix membranes (MMMs) containing organic/inorganic fillers are recommended in this regard. MMMs with more efficient separation, high mechanical strength, good processing ability and long-term stability represent the basic standards for the commercialization of industrial applications [16]. Ismail et al. [17] synthesized polyvinylidene fluoride mixed matrix membranes, including HMO nanoparticles in order to eliminate oils. The obtained results represented that the flux of membranes containing HMO nanoparticles was 10 times greater than that of pure PVDF with an oil separation efficiency of 93%. In another study, Vatanpour et al. [18] synthesized polyethersulfone (PES) based mixed matrix membranes

*Corresponding Author Institutional Email: nimanabian@mazust.ac.ir
(N. Nabian)

using multi-walled carbon nanotubes and titanium oxide coating and then compared them with each other. The results revealed that the hydrophilicity was increased in membranes containing multi-walled carbon nanotubes. Water permeation was also increased significantly in membranes containing carbon nanotubes with titanium oxide coating. Furthermore, Zirepour et al. [19] fabricated a mixed matrix of ultrafiltration membrane containing multi-walled carbon nanotubes. The results showed that these nanotubes had a positive effect on the permeate flux and mechanical strength of the membrane and improved membrane efficiency for the treatment of organic wastewater.

Halloysite nanotubes (HNTs) are more easily modified than other nanomaterials and possess a relatively low price. A group of researchers synthesized a series of novel PES based mixed matrix membranes by blending functionalized HNTs to improve the hydrophilicity and reusability of membranes [20-23]. A utilization of halloysite nanotubes in combination with other nanoparticles as new membrane fillers has been reported in the literature [24]. As an example, Ikhsan et al. [25] investigated the effect of halloysite nanotubes / hydrous iron oxide nanocomposites on a polymer-based composite matrix membrane at different ratios. Their obtained results confirmed that with increasing the nanocomposite up to 23.88 wt%, the contact angle of the membrane decreased from 81.9° to 50.3°. Mixed matrix membranes containing nanoparticles exhibited a water permeation of 650 L.m⁻².h⁻¹ and oil removal efficiency equal to 99.7%. As another candidate to be combined with HNTs, graphene oxide (GO) nanomaterials can improve membrane performance because of their extremely high aspect ratio, excellent hydrophilicity, their easy surface functionalization, and excellent enhancement of membrane properties [26]. Therefore, GO-based membranes incorporated with halloysite nanotubes were prepared for the improvement of membrane separation processes [27]. The results obtained by Zhu et al. [28] demonstrated that by the addition of halloysite nanotubes to polyethersulfone membrane containing GO nanoparticles, the permeate flux was increased from 288.6 L.m⁻².h⁻¹ to 716 L.m⁻².h⁻¹. In addition, some groups of researchers developed a new strategy to improve the performance of HNT/GO membranes through functionalization of halloysite nanotubes via modifiers in order to avoid the accumulation of nanotubes in polymeric solutions [29]. Poly(4-vinylpyridine) (P4VP) was used as a modifier by Zhang et al. [30] to produce a functionalized halloysite nanotubes incorporated in polyethersulfone (PES) based membranes. Zhan et al. [31] fabricated polyarylene ether nitrile (PEN) MMMs for oil removal applications by adding different loadings of polydopamine (PDA) modified halloysite nanotubes to the membranes containing GO nanomaterials. The resulting composite

membranes showed a separation efficiency of more than 99%. In similar studies, the authors changed the ratios of PDA modified halloysite nanotubes to graphene oxide nanoparticles in the cellulose acetate membrane matrix being used in oil/water separation [32-34]. Moreover, it was described elsewhere that sodium dodecyl sulfate (SDS) could be a useful modifier enhancing the dispersion of halloysite nanotubes [1, 2]. Based on the findings reported in the literature, it is not presented anywhere that how the oil/water separation performance of the mixed matrix membranes containing both GO-HNT nanomaterials changes if SDS is used for the functionalization of halloysite nanotubes. Among diverse types of polymers being utilized for the preparation of polymeric membranes, polycarbonate (PC) is an appealing material due to its remarkable features like reasonable chemical stability, good physical toughness, and relatively low price [1, 2]. Therefore, the aim of this study is to prepare polycarbonate based mixed matrix membranes comprising both graphene oxide nanosheets (GO) and sodium dodecyl sulfate functionalized HNTs (FHNT) with three various GO/FHNT ratios. The effects of the simultaneous presence of these hydrophilic nanomaterials on the membrane properties like porosity, mean pore size, and hydrophilicity as well as its performance such as permeability, oil rejection and flux recovery ratio were investigated.

2. MATERIALS AND METHODS

Commercial graphene oxide nanosheets, acetone, polyvinyl pyrrolidone (PVP), N-methyl-2-pyrrolidone (NMP), halloysite nanotubes (HNTs), polycarbonate (grade: 0710), sodium dodecyl sulfate (SDS) and Olive oil was used in this study that introduced mentioned materials in our previous work [35].

2. 1. Preparation of Membranes In this study, four membranes including a pure polycarbonate membrane and three mixed matrix membranes intercalated by both nanomaterials of commercial graphene oxide nanosheets and the functionalized halloysite nanotubes were synthesized in different weight ratios of fillers. The synthesis of functionalized halloysite nanotubes is clearly stated in our previous work [35]. First of all, the predetermined ratios of graphene oxide nanoparticles to functionalized halloysite nanotubes are added to the solution containing NMP and PVP and the resulting mixture was placed on a stirrer at 65°C for 24 hours to completely disperse the nanoparticles into the solution. Then, predetermined amounts of polycarbonate added to the dope solution. The glycerol is then added to the solution and placed on the heater. Thus, the dope solution is prepared for the preparation of MMMs. After spreading the polymeric solution on a flat glass plane, it

was sunk in a cubic container full of water to complete the phase inversion process leading to the formation of the membrane. Later, the synthesis procedure was followed by the detaching the synthesized membrane from the glass plate, the membrane is placed in distilled water. Dope solution ingredients of all fabricated membranes is summarized in Table 1.

2. 2. Characterization Analyses

The transmission electron microscopy (TEM) is a special apparatus for determining the structure and morphology of the synthesized materials, which makes it possible to study the morphological characteristics of samples with high resolution and high magnification. In this study, TEM (Philips, Netherlands) analysis was used to identify the dispersion level as well as the morphology of the functionalized nanotubes. Furthermore, the FESEM apparatus (MIRA3TESCAN-XMU, Czech Republic) was used in this work for the characterization of the commercial HNTs, the modified ones as well as the synthesized membranes. The common feature for most polymers is that they are non-conductive and therefore they definitely need to be coated before implementing this test. In this case, FESEM can be used in low voltage and current conditions. Fourier transform infrared spectroscopy (FTIR) is commonly used to study chemical bonds. The FTIR apparatuses, namely Shimadzu (Japan) and Bomem MB-100 (Canada) were used to determine the presence of the functional groups of the prepared halloysite nanotubes and the fabricated membranes, respectively.

2. 3. Water Contact Angle

By a contact angle measurement system, the hydrophilicity properties of the samples can be investigated. The contact angle refers to the angle that a water droplet makes with a solid surface. With an increase in the wettability feature, the water contact angle decreases. In this study, in order to assess the synthesized membranes' hydrophilicity, the contact angles between water and the membranes' surfaces were obtained using the contact angle measuring instrument (Data physics OCA 15 Plus, Germany). It should be noted that the volume of one drop of water on the membrane surface is equal to 4 microliters. For each

sample, photography was done three times and their average contact angle value was reported.

2. 4. Mechanical Strength

In this study, the mechanical strength tests were done by a universal machine (H10KS, England). Three samples were tested for each membrane and the average tensile strength was reported.

2. 5. Porosity and Mean Pore Size

Porosity is considered as another remarkable index for the evaluation of membrane characteristics. To calculate this parameter, at first, the dry weights of 5 pieces of each membrane (3 cm²) were measured. Then, these pieces of the dry membrane were soaked in distilled water for 48 h. After that, for the removal of extra water from the membrane surface, a filter paper was applied and subsequently weighing the wet membranes was repeated. Finally, the membrane porosity was calculated by Equation (1) and average of them was reported [36]:

$$\varepsilon = \frac{\frac{m_{wet} - m_{dry}}{\rho_{water}}}{\frac{m_{wet} - m_{dry}}{\rho_{water}} + \frac{m_{dry}}{\rho_{PC}}} \quad (1)$$

where m_{dry} is the weight of dry membrane and m_{wet} is the wet one (g). ρ_{PC} and ρ_{water} represent the density of polycarbonate (1.22 g/cm³) and that of water (0.998 g/cm³), respectively.

Also, the following equation was used for the calculation of membrane mean pore size [37]:

$$r_{average} = \sqrt{\frac{8\mu l q (2.9 - 1.75\varepsilon)}{\varepsilon A \Delta P}} \quad (2)$$

where μ refers to the viscosity of water at 25 °C in Pascal-seconds, l represents thickness of fabricated membranes in meter, q refers to water flow in cubic meters per seconds, ΔP represents the atmospheric operation pressure in Pascal, and A refers to surface area of membrane in square meters.

2. 6. Water Permeation

Water permeation (J in L.m⁻².h⁻¹) was calculated by Equation (3) [38]:

$$J = \frac{Q}{A \Delta t} \quad (3)$$

where Q shows the volume of collected permeate in liter, Δt refers to the duration of permeate collection in hour. Meanwhile, the pressures used to achieve the membrane water permeation were 1, 1.5, and 2 bar. It is notable that to measure the permeate flux and oil removal efficiency of synthesized membranes an ultrafiltration setup was applied. The process diagram of this setup is shown in previous work schematically [35].

2. 7. Oil Removal Efficiency

To measure the efficiency of membranes in olive oil/aqueous solution separation, at first, the membrane was used for thirty

TABLE 1. Dope solution ingredients of prepared membranes

Membrane code	PC (wt%)	NMP (wt%)	PVP (wt%)	Glycerol (wt%)	GO (wt%)	FHNT (wt%)
Pristine PC	12	82.13	5	0.87	0	0
GO0.25-FHNT0.75	12	81.13	5	0.87	0.25	0.75
GO0.5-FHNT0.5	12	81.13	5	0.87	0.5	0.5
GO0.75-FHNT0.25	12	81.13	5	0.87	0.75	0.25

minutes where the tank in the ultrafiltration set-up was filled with deionized water to minimize the effects of membrane compactness. Then, the tests continued in which an emulsion of olive oil in water flowed through the UF setup instead of water. In this test, although the concentration of feed solution varied, the other feed parameters were remained unchanged like the pressure of 1 bar and the flow rate of 1 L/min. Using Equation (4), the efficiency of membranes in the removal of olive oil (R in percent form) was estimated [39]:

$$R = \frac{C_F - C_P}{C_F} \quad (4)$$

where C_P and C_F represent the olive oil concentration in the collected permeate and feed tank, respectively.

2. 8. Antifouling Tests The optimum was reused to antifouling test. For this purpose, the pure water flux of membrane was measured again (J_2). After that, the flux recovery ratio (FRR) of the optimal membrane was calculated by Equation (5) [40]:

$$FRR = \frac{J_2}{J_1} \times 100 \quad (5)$$

where J_2 and J_1 ($L \cdot m^{-2} \cdot h^{-1}$) refer to the water permeation of the membrane after and before the oil removal test, respectively.

3. RESULTS AND DISCUSSION

3. 1. Characterization of Graphene Oxide Nanomaterials and Functionalized Halloysite Nanotubes

3. 1. 1. FESEM The FESEM images of HNTs and functionalized ones are displayed in Figures 1A and 1B, respectively. It can be confirmed that the HNTs are aggregated, while the FHNTs are in a uniform distribution of nanotubes as well as a decrease in their particle size.

3. 1. 2. TEM Analysis Results of TEM analysis for FHNTs and GO are shown in Figures 2A, and 2B, respectively. Figure 2A represents the tubular structure of functionalized halloysite nanotubes at different magnifications. Similar findings were reported by Lun et al. [2]. In a study conducted by Cheng et al. [41] the functionalized halloysite nanotubes with sodium dodecyl sulfate showed much lower agglomeration and more uniform distribution. Moreover, based on Figure 2B, the surface roughness and amorphous structure of the graphene oxide nanomaterials can be observed [42].

3. 1. 3. FTIR Analysis of FHNTs The FTIR spectra of functionalized halloysite nanotubes are discussed in

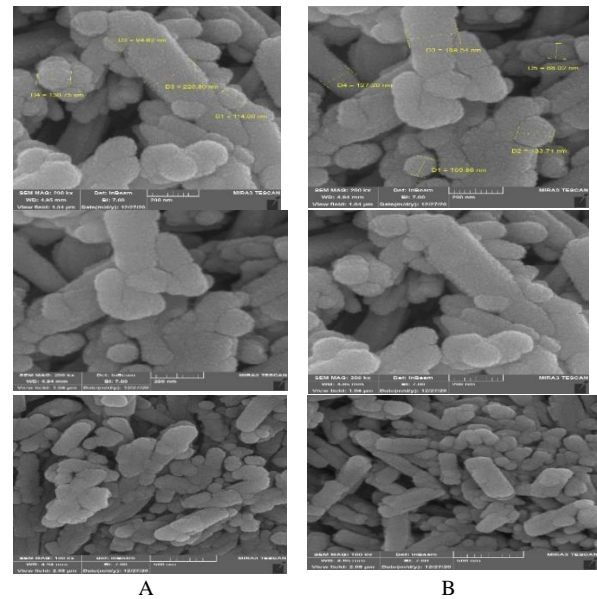


Figure 1. FESEM images of A) Commercial HNTs, B) Functionalized HNTs

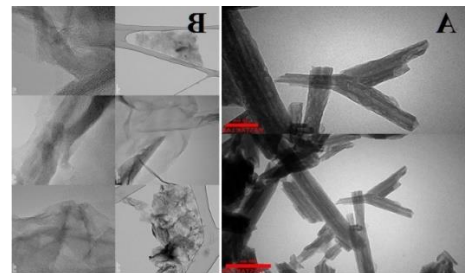


Figure 2. TEM analysis of A) Functionalized halloysite nanotubes and B) GO nanomaterials

our previous study [35]. Briefly, the five peaks confirming the presence of sodium dodecyl sulfate appeared in the FTIR image of sodium dodecyl sulfate functionalized halloysite nanotubes.

3. 2. Characterization of Synthesized Pristine PC and MMMs

3. 2. 1. Morphology of Membranes The upside surface and cross-sectional FESEM results of the blank PC and GO0.25-FHNT0.75 mixed matrix membranes are shown in Figures 3a and 3b, respectively.

By comparing Figures 3a and 3b, it can be seen that the membrane containing nanoparticles has a more spongy structure than the pure polycarbonate membrane. This result can be attributed to the bonds between nanoparticles and the membrane matrix. Various studies have shown that created bonds can affect the mixing process [43]. The reduction in the rate of replacement between coagulant and solvent in the synthesis process of mixed matrix membranes, created membranes with a

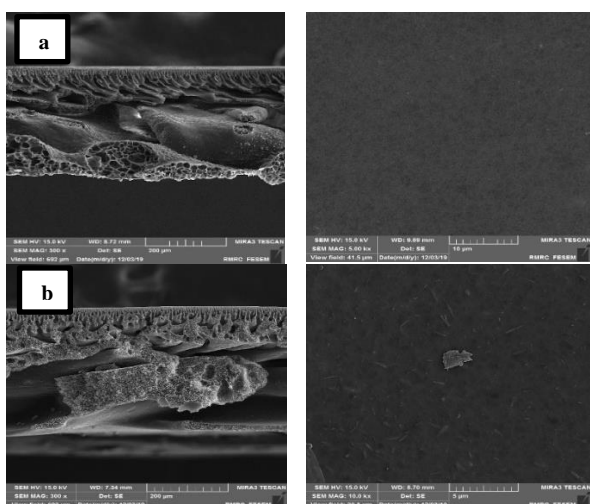


Figure 3. Cross section and top surface of a) blank PC b) GO-FHNT0.75 mixed matrix membrane

more spongy structure than blank membrane [44]. Also, by addition of functionalized HNTs and GO nanomaterials results in the formation of the larger macro-pores in the sub-layer of the membrane, which can be due to the fact that the functionalized HNTs and GO nanomaterials are naturally hydrophilic [45-47]. Furthermore, the top layer of the blank PC has a uniform and smooth surface. But, referring to the upside surface image of GO0.25-FHNT0.75 mixed matrix membrane, GO nanosheets in the center of the picture as well as uniformly distributed nanotubes (FHNTs) can be seen, which verifies the presence of both nanomaterials.

3. 2. 2. Functional Groups The results of FTIR analysis is presented in Figure 4. The functional groups of blank PC and mixed matrix membranes containing GO and FHNTs were in detail discussed in our previous work [35, 47]. In brief, the peaks at 1081 cm^{-1} , 1260 cm^{-1} , 1365 cm^{-1} , 1466 cm^{-1} , 1505 cm^{-1} , 1772 cm^{-1} , and 2854 cm^{-1} correspond to the vibrations of chemical bonds in the blank polycarbonate membrane. The peak appeared at 3465 cm^{-1} is related to adsorbed water. Furthermore, the peaks at 1241 cm^{-1} , 1466 cm^{-1} , and 2922 cm^{-1} are attributed to the presence of functionalized HNTs in the membrane matrix. The bond between SDS-HNTs and PC polymeric material can be assigned to the hydrogen bond between the surface hydroxyl group of the HNTs and the carbonyl group of polycarbonate as well as the hydrophobic-hydrophobic interaction between the alkyl chain of SDS molecules and the benzene ring present in the polycarbonate matrix. The peaks appeared at 1037 cm^{-1} , 1056 cm^{-1} , 1380 cm^{-1} , 1631 cm^{-1} , and 1729 cm^{-1} , and 3433 cm^{-1} are assigned to different functional groups of GO nanosheets.

3. 2. 3. Mechanical Strength The results of mechanical strength of prepared membranes are shown

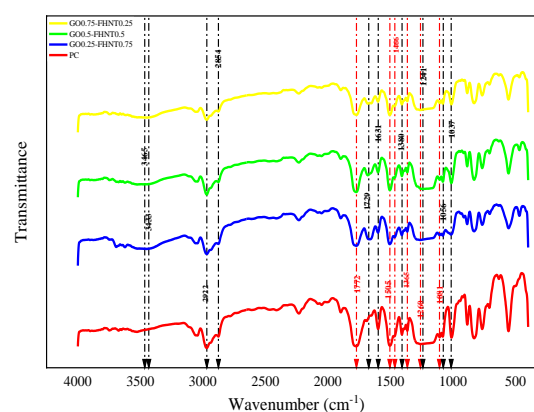


Figure 4. FTIR spectra of blank PC and mixed matrix membranes

in Figure 5. It can be confirmed that addition of nanomaterials, increased the tensile strength and Young's modulus and elongation increased. It can be related to the presence of epoxide functional groups in GO nanomaterials [48]. On the other hand, when the GO loading increased to 0.75 wt%, these mechanical parameters exhibited a decreasing trend. It can be related to the agglomeration of nanosheets in the polymeric solution. In similar studies, the same results were reported [49-50]. Moreover, although GO0.75-FHNT0.25 possessed a GO loading of more than 0.5 wt% after which the mechanical parameters decreased, it still exhibited tensile strength and elongation values greater than those of GO0.25-FHNT0.75 MMM. It can be attributed to the better dispersion of functionalized halloysite nanotubes and a stronger bond between functionalized halloysite nanotubes and polymeric matrix [51].

3. 2. 4. Hydrophilicity Figure 6 shows the contact angle of synthesized membranes. The obtained results confirm that adding GO nanomaterials and FHNTs

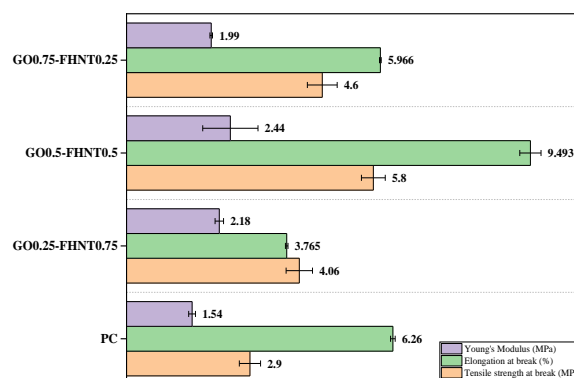


Figure 5. Mechanical strength of mixed matrix membranes

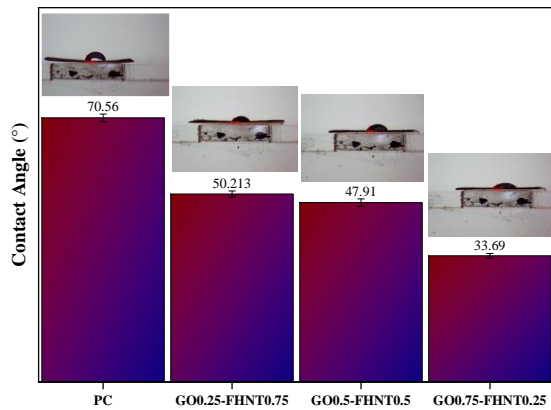


Figure 6. Water contact angle of synthesized membrane

enhanced the hydrophilicity of mixed matrix membranes in comparison with that of blank PC membrane. It can be attributed to the hydrophilic groups attached on GO and FHNTs. Also, SDS as amphiphilic material, could produce a large amount of hydrophilic cavity and functional groups of functionalized halloysite nanotubes [52].

3. 2. 5. Porosity and Mean Pore Size

The porosity and mean pore size of synthesized membranes are presented in Figure 7. As shown in Figure 7, the porosity quantities of mixed matrix membranes were bigger than that value achieved for the pure polycarbonate membrane. Also, by increasing the loadings of GO nanomaterials, porosity values reduced. In can be due to a rise in the viscosity of the polymeric solution, as a result of a reduction in the substitution rate of coagulant and solvent in the phase inversion procedure [53, 54]. In addition, because of the tubular structure of halloysite nanotubes, they make the membranes porous after being dispersed in the dope solution [35, 55].

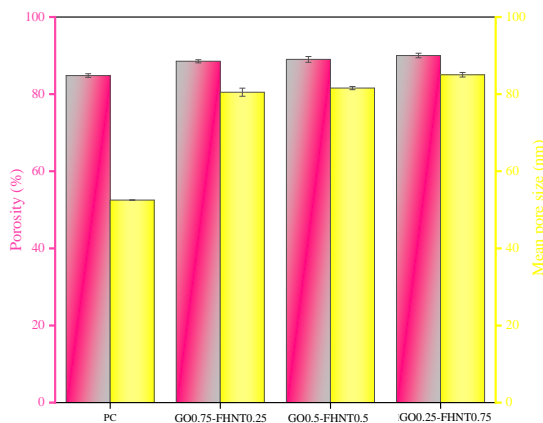


Figure 7. Porosity and mean pore size of membranes

The overall results of membranes mean pore size confirmed that mean pore sizes of mixed matrix membranes were more than that of the pure membrane. But, an enhancement in the loading of GO nanomaterials shows a negative effect on the mean pore size because of strong hydrogen bonds between GO nanosheets and the polymeric solution [42].

3. 2. 6. Ultrafiltration Experiments

For the investigation of the performance of synthesized membranes, some tests were carried out using the ultrafiltration setup such as water permeation, oil separation, and membrane regeneration that will be described in the following sections.

3. 2. 6. 1. Water Permeation

Regarding the obtained results of water permeation displayed in Figure 8, the water permeation of mixed matrix membranes improved around 3 times in comparison to blank PC. It can be due to the hydrophilic nature of these added nanomaterials. In addition, the enhancement in the water permeation of GO0.25-FHNT0.75 compared with GO0.75-FHNT0.25 from 1237.5 L.m⁻².h⁻¹ to 1025 L.m⁻².h⁻¹ can be attributed to the greater hydrophilicity of halloysite nanotubes and its hollow tubular structure that offers a wide range of channels for water permeation [55-57] as well as the agglomeration of GO nanomaterials [58-60]. Based on these obtained data of water permeation as well as porosity and water contact angle values, GO0.25-FHNT0.75 mixed matrix membrane selected as the optimal membrane.

3. 2. 6. 2. Oil Separation of Selected Membranes

The effect of feed concentration on the separation efficiency of olive oil by the optimal membrane in ultrafiltration tests at 1 bar and ambient temperature was investigated and the results are shown in Figures 9. For this purpose, the feed solution was prepared in 100-200

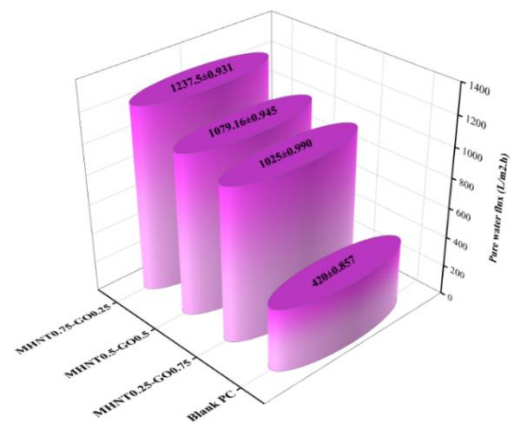


Figure 8. Water permeation of blank PC and mixed matrix membranes

ppm oil concentrations, and subsequently the selected membrane was examined for the efficiency of olive oil separation using the as-prepared feed solution.

To interpret the results displayed in Figure 9, this point is noteworthy that as the UF process begins, the presence of quite open membrane pores allows some oil particles to come out from the other side of the membrane. Over time, some pores become blocked with oil particles, and as a result, oil separation efficiency

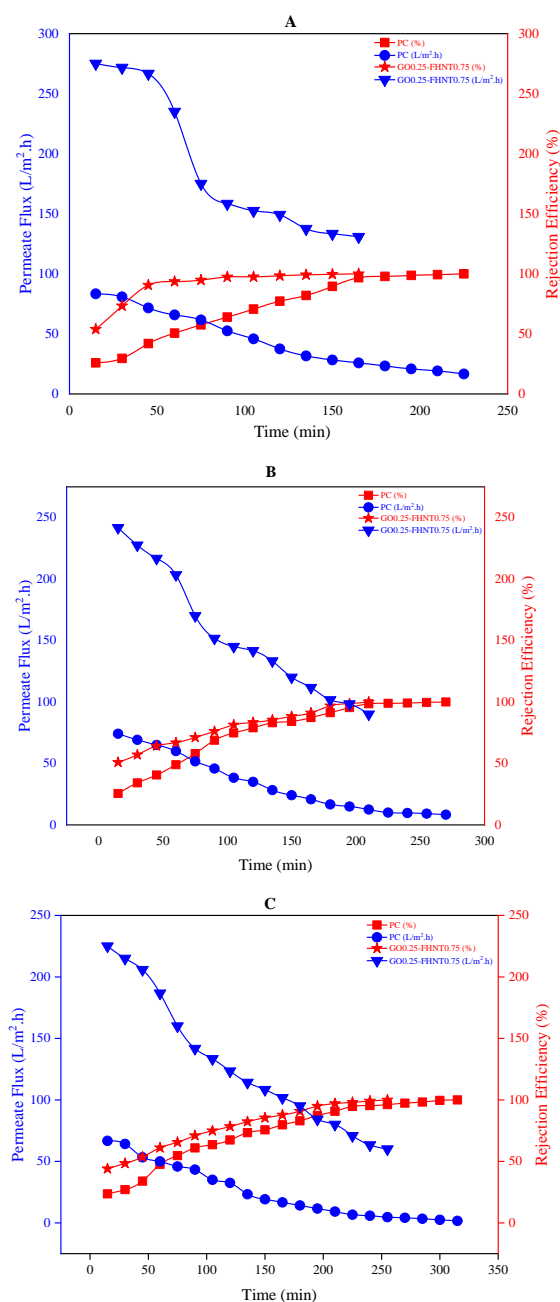


Figure 9. Permeate flux and separation efficiency of blank PC and the optimal mixed matrix membrane at A) 100 ppm, B) 150 ppm, C) 200 ppm, 1 bar and 25°C

increases up to 100%. But, the times to reach this separation efficiency decreased from 225 min for the blank PC to 165 minutes for the GO0.25-FHNT0.75 membrane at 100 ppm feed concentration. Also, with increasing the concentration of the feed solution, the time to achieve 100% separation increased. In addition, for the investigation of membrane fouling, the curves of permeate flux versus time are plotted in Figures 9A, 9B and 9C for each feed concentration. In detail, the blank PC membrane possessed the lower permeate flux compared with the optimal GO0.25-FHNT0.75 MMM.

3. 2. 6. 3. Reusability of Optimal Membrane

After ultrafiltration experiments, the optimal membrane was used in reusability test and the results were plotted in Figure 10. In other words, GO0.25-FHNT0.75 mixed matrix membrane was evaluated in terms of regeneration. In this case, the used membrane was washed after oil separation ultrafiltration tests by acetone solution (20% v/v). After that, the water permeation of washed membrane was measured again. This method was repeated for three times. Finally, the flux recovery ratio was calculated by Equation (5). The obtained results showed that with increasing feed concentration, the FRR decreased [35, 47]. It can be due to the blockage of some pores and not complete cleaning of membrane pores by acetone solution. Furthermore, the permeate fluxes of feed solutions with 100 ppm and 200 ppm olive oil concentrations were reduced only about 5.5% and 6% after three cycles, respectively [61].

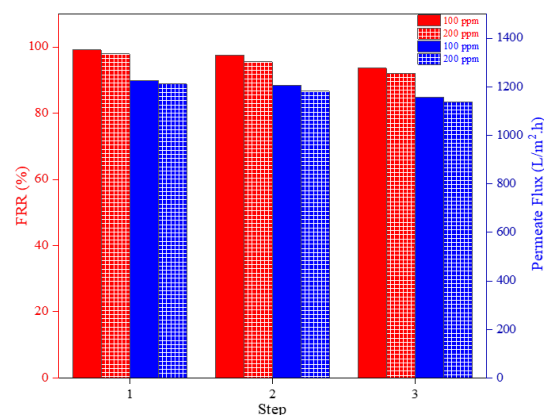


Figure 10. FRR results of GO0.25-FHNT0.75 mixed matrix membrane

4. CONCLUSION

In this work, polycarbonate membranes were synthesized in which the functionalized HNTs and GO nanomaterials were added in the dope solution of the membrane simultaneously. According to the FESEM images, the mixed matrix membrane showed a more spongy structure

compared to the blank PC membrane. In addition, the water permeation results showed that the best wettability was related to GO0.25-FHNT0.75 mixed matrix membrane.

Also, water contact angle of FHNT/GO membrane compared to blank PC membrane decreased from 70.56° to 33.69°. As a result, water permeation of FHNT/GO mixed matrix membrane increased by 2.9 times compared to blank PC membrane.

The overall results of mean pore size of membranes confirmed that the mean pore size of FHNT/GO mixed matrix membranes increased about 1.5 times compared to blank PC membrane.

The pure polycarbonate membrane and the optimum GO0.25-FHNT0.75 mixed matrix membrane were used for ultrafiltration experiments of olive oil removal from water. The UF results confirmed that synthesized membranes had a desirable ability for olive oil removal up to 100% separation efficiency. Finally, the reusability of GO0.25-FHNT0.75 membrane was checked and the obtained data confirmed that the mentioned membrane was well regenerated with a flux recovery ratio of more than 93% after three cycles.

5. REFERENCES

- Cheng, Z.-L., Chang, X.-Y., Liu, Z. and Qin, D.-Z., "Surface-modified halloysite nanotubes as fillers applied in reinforcing the performance of polytetrafluoroethylene-zinc lin cheng et al. Surface-modified hnts applied in ptfe", *Clay Minerals*, Vol. 53, No. 4, (2018), 643-656. <https://doi.org/10.1180/clm.2018.48>
- Lun, H., Ouyang, J. and Yang, H., "Enhancing dispersion of halloysite nanotubes via chemical modification", *Physics and Chemistry of Minerals*, Vol. 41, No. 4, (2014), 281-288. <https://doi.org/10.1007/s00269-013-0646-9>
- Moghadassi, A., Hamidi, A., Hosseini, S. and Bagheripour, E., "Fabrication and characterization of novel mixed matrix polyethersulfone based nanofiltration membrane modified by ilmenite", *International Journal of Engineering, Transactions A: Basics*, Vol. 30, No. 1, (2017), 7-14. doi: 10.5829/idosi.ije.2017.30.01a.02
- Gude, V.G., "Desalination and sustainability—an appraisal and current perspective", *Water Research*, Vol. 89, (2016), 87-106. <https://doi.org/10.1016/j.watres.2015.11.012>
- Obotey Ezugbe, E. and Rathilal, S., "Membrane technologies in wastewater treatment: A review", *Membranes*, Vol. 10, No. 5, (2020), 89. <https://doi.org/10.3390/membranes10050089>
- Abadi, S.R.H., Sebzari, M.R., Hemati, M., Rekabdar, F. and Mohammadi, T., "Ceramic membrane performance in microfiltration of oily wastewater", *Desalination*, Vol. 265, No. 1-3, (2011), 222-228. <https://doi.org/10.1016/j.desal.2010.07.055>
- Akhaier, S., Harun, Z., Basri, H., Ahmad, R., Rashid, A. and Azhar, F.H., "Hydrophobicity properties of graphite and reduced graphene oxide of the polysulfone (PSF) mixed matrix membrane", *International Journal of Engineering, Transactions B: Applications*, Vol. 31, No. 8, (2018), 1381-1388. doi: 10.5829/ije.2018.31.08b.29
- Gholami, F., Zinadini, S., Zinatizadeh, A., Noori, E. and Rafiee, E., "Preparation and characterization of an antifouling polyethersulfone nanofiltration membrane blended with graphene oxide/ag nanoparticles", *International Journal of Engineering, Transactions A: Basics*, Vol. 30, No. 10, (2017), 1425-1433. doi: 10.5829/ije.2017.30.10a.02
- Delavar, M., Bakeri, G. and Hosseini, M., "Fabrication of polycarbonate mixed matrix membranes containing hydrous manganese oxide and alumina nanoparticles for heavy metal decontamination: Characterization and comparative study", *Chemical Engineering Research and Design*, Vol. 120, (2017), 240-253. <https://doi.org/10.1016/j.cherd.2017.02.029>
- Lively, R.P. and Sholl, D.S., "From water to organics in membrane separations", *Nature Materials*, Vol. 16, No. 3, (2017), 276-279. <https://doi.org/10.1038/nmat4860>
- Bagheri, M., Sangpour, P., Badiei, E. and Pazouki, M., "Graphene oxide antibacterial sheets: Synthesis and characterization (research note)", *International Journal of Engineering, Transactions C: Aspects*, Vol. 27, No. 12, (2014), 1803-1808. doi: 10.5829/idosi.ije.2014.27.12c.01
- Cai, Y., Chen, D., Li, N., Xu, Q., Li, H., He, J. and Lu, J., "Nanofibrous metal-organic framework composite membrane for selective efficient oil/water emulsion separation", *Journal of Membrane Science*, Vol. 543, (2017), 10-17. <https://doi.org/10.1016/j.memsci.2017.08.047>
- Chen, W., Su, Y., Zheng, L., Wang, L. and Jiang, Z., "The improved oil/water separation performance of cellulose acetate-graft-polyacrylonitrile membranes", *Journal of Membrane Science*, Vol. 337, No. 1-2, (2009), 98-105. <https://doi.org/10.1016/j.memsci.2009.03.029>
- Zinadini, S., Moradi, M., and Zinatizadeh, A. A. L. "Influence of operating variables on performance of nanofiltration membrane for dye removal from synthetic wastewater using response surface methodology" *International Journal of Engineering, Transactions C: Aspects*, Vol. 29, No. 12, (2016), 1650-1658. doi: 10.5829/idosi.ije.2016.29.12c.03
- Mohammadipour, E., Nabian, N. and Delavar, M., "Novel pvc-melamine mixed matrix membranes for the sirius red removal from aqueous solutions: Experimental study and rsm modeling", *Journal of Water Process Engineering*, Vol. 47, (2022), 102752. <https://doi.org/10.1016/j.jwpe.2022.102752>
- Li, Y.S., Yan, L., Xiang, C.B. and Hong, L.J., "Treatment of oily wastewater by organic-inorganic composite tubular ultrafiltration (UF) membranes", *Desalination*, Vol. 196, No. 1-3, (2006), <https://doi.org/10.1016/j.desal.2005.11.021>
- Ismail, N., Salleh, W., Awang, N., Ahmad, S., Rosman, N., Sazali, N. and Ismail, A., "Pvdf/hmo ultrafiltration membrane for efficient oil/water separation", *Chemical Engineering Communications*, Vol. 208, No. 4, (2021), 463-473. <https://doi.org/10.1080/00986445.2019.1650035>
- Vatanpour, V., Madaeni, S.S., Moradian, R., Zinadini, S. and Astinchap, B., "Novel antibifouling nanofiltration polyethersulfone membrane fabricated from embedding tio2 coated multiwalled carbon nanotubes", *Separation and Purification Technology*, Vol. 90, (2012), 69-82. <https://doi.org/10.1016/j.seppur.2012.02.014>
- Zirehpour, A., Rahimpour, A., Jahanshahi, M. and Peyravi, M., "Mixed matrix membrane application for olive oil wastewater treatment: Process optimization based on taguchi design method", *Journal of Environmental Management*, Vol. 132, (2014), 113-120. <https://doi.org/10.1016/j.jenvman.2013.10.028>
- Lannelongue, G., Gonzalez-Benito, J. and Quiroz, I., "Environmental management and labour productivity: The moderating role of capital intensity", *Journal of Environmental Management*, Vol. 190, (2017), 158-169. <https://doi.org/10.1016/j.jenvman.2016.11.051>
- Yu, L., Zhang, Y., Zhang, H. and Liu, J., "Development of a molecular separation membrane for efficient separation of low-molecular-weight organics and salts", *Desalination*, Vol. 359, (2015), 176-185. <https://doi.org/10.1016/j.desal.2014.12.044>

22. Wei, A., Liu, B., Zhao, H., Chen, Y., Wang, W., Ma, Y., Yang, H. and Liu, S., "Synthesis and formation mechanism of flowerlike architectures assembled from ultrathin nio nanoflakes and their adsorption to malachite green and acid red in water", *Chemical Engineering Journal*, Vol. 239, (2014), 141-148. <https://doi.org/10.1016/j.cej.2013.10.079>
23. Costa, E.P., Roccamante, M., Amorim, C.C., Oller, I., Pérez, J.A.S. and Malato, S., "New trend on open solar photoreactors to treat micropollutants by photo-fenton at circumneutral ph: Increasing optical pathway", *Chemical Engineering Journal*, Vol. 385, (2020), 123982. <https://doi.org/10.1016/j.cej.2019.123982>
24. Zhu, L., Wang, H., Bai, J., Liu, J. and Zhang, Y., "A porous graphene composite membrane intercalated with halloysite nanotubes for efficient dye desalination", *Desalination*, Vol. 420, (2017), 145-157. <https://doi.org/10.1016/j.desal.2017.07.008>
25. Ikhsan, S.N.W., Yusof, N., Aziz, F., Misdan, N., Ismail, A.F., Lau, W.-J., Jaafar, J., Salleh, W.N.W. and Hairom, N.H.H., "Efficient separation of oily wastewater using polyethersulfone mixed matrix membrane incorporated with halloysite nanotube-hydrous ferric oxide nanoparticle", *Separation and Purification Technology*, Vol. 199, (2018), 161-169. <https://doi.org/10.1016/j.seppur.2018.01.028>
26. Yang, L., Tang, B. and Wu, P., "Uf membrane with highly improved flux by hydrophilic network between graphene oxide and brominated poly (2, 6-dimethyl-1, 4-phenylene oxide)", *Journal of Materials Chemistry A*, Vol. 2, No. 43, (2014), 18562-18573. <https://doi.org/10.1039/C4TA03790A>
27. Lim, S., Park, M.J., Phuntsho, S., Mai-Prochnow, A., Murphy, A.B., Seo, D. and Shon, H., "Dual-layered nanocomposite membrane incorporating graphene oxide and halloysite nanotube for high osmotic power density and fouling resistance", *Journal of Membrane Science*, Vol. 564, (2018), 382-393. <https://doi.org/10.1016/j.memsci.2018.06.055>
28. Zhu, Y., Chen, P., Nie, W. and Zhou, Y., "Greatly improved oil-in-water emulsion separation properties of graphene oxide membrane upon compositing with halloysite nanotubes", *Water, Air, & Soil Pollution*, Vol. 229, No. 3, (2018), 1-9. <https://doi.org/10.1007/s11270-018-3757-6>
29. Zeng, G., He, Y., Ye, Z., Yang, X., Chen, X., Ma, J. and Li, F., "Novel halloysite nanotubes intercalated graphene oxide based composite membranes for multifunctional applications: Oil/water separation and dyes removal", *Industrial & Engineering Chemistry Research*, Vol. 56, No. 37, (2017), 10472-10481. <https://doi.org/10.1021/acs.iecr.7b02723>
30. Zhang, J., Zhang, Y., Chen, Y., Du, L., Zhang, B., Zhang, H., Liu, J. and Wang, K., "Preparation and characterization of novel polyethersulfone hybrid ultrafiltration membranes bending with modified halloysite nanotubes loaded with silver nanoparticles", *Industrial & Engineering Chemistry Research*, Vol. 51, No. 7, (2012), 3081-3090. <https://doi.org/10.1021/ie202473u>
31. Zhan, Y., He, S., Wan, X., Zhao, S. and Bai, Y., "Thermally and chemically stable poly (arylene ether nitrile)/halloysite nanotubes intercalated graphene oxide nanofibrous composite membranes for highly efficient oil/water emulsion separation in harsh environment", *Journal of Membrane Science*, Vol. 567, (2018), 76-88. <https://doi.org/10.1016/j.memsci.2018.09.037>
32. Li, F., Yu, Z., Shi, H., Yang, Q., Chen, Q., Pan, Y., Zeng, G. and Yan, L., "A mussel-inspired method to fabricate reduced graphene oxide/g-c3n4 composites membranes for catalytic decomposition and oil-in-water emulsion separation", *Chemical Engineering Journal*, Vol. 322, (2017), 33-45. <https://doi.org/10.1016/j.cej.2017.03.145>
33. Di Luccio, M., Nobrega, R. and Borges, C.P., "Microporous anisotropic phase inversion membranes from bisphenol a polycarbonate: Effect of additives to the polymer solution", *Journal of Applied Polymer Science*, Vol. 86, No. 12, (2002), 3085-3096. <https://doi.org/10.1002/app.11338>
34. Feng, J., Hao, J., Du, J. and Yang, R., "Using tga/fir tga/ms and cone calorimetry to understand thermal degradation and flame retardancy mechanism of polycarbonate filled with solid bisphenol a bis (diphenyl phosphate) and montmorillonite", *Polymer Degradation and Stability*, Vol. 97, No. 4, (2012), 605-614. <https://doi.org/10.1016/j.polymdegradstab.2012.01.011>
35. Amid, M., Nabian, N. and Delavar, M., "Fabrication of polycarbonate ultrafiltration mixed matrix membranes including modified halloysite nanotubes and graphene oxide nanosheets for olive oil/water emulsion separation", *Separation and Purification Technology*, Vol. 251, (2020), 117332. <https://doi.org/10.1016/j.seppur.2020.117332>
36. Delavar, M., Bakeri, G., Hosseini, M. and Nabian, N., "Fabrication and characterization of polyvinyl chloride mixed matrix membranes containing high aspect ratio anatase titania and hydrous manganese oxide nanoparticle for efficient removal of heavy metal ions: Competitive removal study", *The Canadian Journal of Chemical Engineering*, Vol. 98, No. 7, (2020), 1558-1579. <https://doi.org/10.1002/cjce.23725>
37. Yuliwati, E., Ismail, A., Matsuura, T., Kassim, M. and Abdullah, M., "Effect of modified pvdf hollow fiber submerged ultrafiltration membrane for refinery wastewater treatment", *Desalination*, Vol. 283, (2011), 214-220. <https://doi.org/10.1016/j.desal.2011.03.049>
38. Yuan, X., Li, W., Zhu, Z., Han, N. and Zhang, X., "Thermo-responsive pvdf/psma composite membranes with micro/nanoscale hierarchical structures for oil/water emulsion separation", *Colloids and Surfaces A: Physicochemical and Engineering Aspects*, Vol. 516, (2017), 305-316. <https://doi.org/10.1016/j.colsurfa.2016.12.047>
39. Saadati, J. and Pakizeh, M., "Separation of oil/water emulsion using a new psf/pebax/f-mwcnt nanocomposite membrane", *Journal of the Taiwan Institute of Chemical Engineers*, Vol. 71, (2017), 265-276. <https://doi.org/10.1016/j.jtice.2016.12.024>
40. Safarpour, M., Khataee, A. and Vatanpour, V., "Preparation of a novel polyvinylidene fluoride (PVDF) ultrafiltration membrane modified with reduced graphene oxide/titanium dioxide (tio2) nanocomposite with enhanced hydrophilicity and antifouling properties", *Industrial & Engineering Chemistry Research*, Vol. 53, No. 34, (2014), 13370-13382. <https://doi.org/10.1021/ie502407g>
41. Cheng, Z.-L., Chang, X.-Y. and Liu, Z., "Surface modification of halloysite nanotubes grafted by dodecylamine and their application in reinforcing polytetrafluoroethylene", *Clay Minerals*, Vol. 54, No. 2, (2019), 219-225. <https://doi.org/10.1180/clm.2019.29>
42. Nasirizadeh, N., Ghaani, M., Shekari, Z. and Shateri-Khalilabad, M., "Novel non enzymatic tbhq modified electrochemical sensor for hydrogen peroxide determination in different beverage samples", *Journal of the Brazilian Chemical Society*, Vol. 27, (2016), 1577-1586. <https://doi.org/10.5935/0103-5053.20160037>
43. Chang, X., Wang, Z., Quan, S., Xu, Y., Jiang, Z. and Shao, L., "Exploring the synergetic effects of graphene oxide (go) and polyvinylpyrrolidone (PVP) on poly (vinylidene fluoride)(pvdf) ultrafiltration membrane performance", *Applied Surface Science*, Vol. 316, (2014), 537-548. <https://doi.org/10.1016/j.apsusc.2014.07.202>
44. Zinatadini, S., Zinatizadeh, A.A., Rahimi, M., Vatanpour, V. and Zangeneh, H., "Preparation of a novel antifouling mixed matrix pes membrane by embedding graphene oxide nanoplates", *Journal of Membrane Science*, Vol. 453, (2014), 292-301. <https://doi.org/10.1016/j.memsci.2013.10.070>
45. Narasimha Rao, C., Subbarayudu, K., Vijaya, Y. and Venkata Subbaiah, M., "Adsorption of ni (ii) from aqueous solution by

- activated carbons derived from tobacco stem", *Desalination and Water Treatment*, Vol. 54, No. 12, (2015), 3392-3399. <https://doi.org/10.1080/19443994.2014.910837>
46. Wang, Z., Yu, H., Xia, J., Zhang, F., Li, F., Xia, Y. and Li, Y., "Novel go-blended pvdf ultrafiltration membranes", *Desalination*, Vol. 299, (2012), 50-54. <https://doi.org/10.1016/j.desal.2012.05.015>
 47. Amid, M., Nabian, N. and Delavar, M., "Performance evaluation and modeling study of pc blended membranes incorporated with sds-modified and unmodified halloysite nanotubes in the separation of oil from water", *Journal of Environmental Chemical Engineering*, Vol. 9, No. 4, (2021), 105237. <https://doi.org/10.1016/j.jece.2021.105237>
 48. Nasir, M., "Graphene Based Membrane Modified Silica Nanoparticles (GO/SiO₂-Psf) for Seawater Desalination and Wastewater Treatment: Salt Rejection and Dyes" *International Journal of Engineering, Transactions A: Basics*, Vol. 36, No. 4, (2023), 698-708, doi: 10.5829/ije.2023.36.04a.09
 49. Qi, B., Lu, S., Xiao, X., Pan, L., Tan, F. and Yu, J., "Enhanced thermal and mechanical properties of epoxy composites by mixing thermotropic liquid crystalline epoxy grafted graphene oxide", *Express Polymer Letters*, Vol. 8, No. 7, (2014). DOI: 10.3144/expresspolymlett.2014.51
 50. Shen, X.-J., Liu, Y., Xiao, H.-M., Feng, Q.-P., Yu, Z.-Z. and Fu, S.-Y., "The reinforcing effect of graphene nanosheets on the cryogenic mechanical properties of epoxy resins", *Composites Science and Technology*, Vol. 72, No. 13, (2012), 1581-1587. <https://doi.org/10.1016/j.compscitech.2012.06.021>
 51. Foorginejad, A., Taheri, M., & Mollayi, N., "A non-destructive ultrasonic testing approach for measurement and modelling of tensile strength in rubbers", *International Journal of Engineering, Transactions C: Aspects*, Vol. 33, No. 12, (2020), 2549-2555. doi: 10.5829/ije.2020.33.12c.16
 52. Saif, M.J., Asif, H.M. and Naveed, M., "Properties and modification methods of halloysite nanotubes: A state-of-the-art review", *Journal of the Chilean Chemical Society*, Vol. 63, No. 3, (2018), 4109-4125. <http://dx.doi.org/10.4067/s0717-97072018000304109>
 53. Gianni, E., Avgoustakis, K., Pšenička, M., Pospíšil, M. and Papoulis, D., "Halloysite nanotubes as carriers for irinotecan: Synthesis and characterization by experimental and molecular simulation methods", *Journal of Drug Delivery Science and Technology*, Vol. 52, (2019), 568-576. <https://doi.org/10.1016/j.jddst.2019.05.001>
 54. Han, M.-J. and Nam, S.-T., "Thermodynamic and rheological variation in polysulfone solution by pvp and its effect in the preparation of phase inversion membrane", *Journal of Membrane Science*, Vol. 202, No. 1-2, (2002), 55-61. [https://doi.org/10.1016/S0376-7388\(01\)00718-9](https://doi.org/10.1016/S0376-7388(01)00718-9)
 55. Liang, W., Ge, X., Ge, J., Li, T., Zhao, T., Chen, X., Song, Y., Cui, Y., Khan, M. and Ji, J., "Reduced graphene oxide embedded with mq silicone resin nano-aggregates for silicone rubber composites with enhanced thermal conductivity and mechanical performance", *Polymers*, Vol. 10, No. 11, (2018), 1254. <https://doi.org/10.3390/polym10111254>
 56. Ng, E.-P., Subari, S.N.M., Marie, O., Mukti, R.R. and Juan, J.-C., "Sulfonic acid functionalized mcm-41 as solid acid catalyst for tert-butylolation of hydroquinone enhanced by microwave heating", *Applied Catalysis A: General*, Vol. 450, (2013), 34-41. <https://doi.org/10.1016/j.apcata.2012.09.055>
 57. Farokhi, B., Rezaei, M., Kiamehr, Z. and Hosseini, S., "A new approach to provide high water permeable polyethersulfone based nanofiltration membrane by air plasma treatment", *International Journal of Engineering, Transactions C: Aspects*, Vol. 32, No. 3, (2019), 354-359. doi: 10.5829/ije.2019.32.03c.01
 58. Yuan, P., Southon, P.D., Liu, Z., Green, M.E., Hook, J.M., Antill, S.J. and Kepert, C.J., "Functionalization of halloysite clay nanotubes by grafting with γ -aminopropyltriethoxysilane", *The Journal of Physical Chemistry C*, Vol. 112, No. 40, (2008), 15742-15751. <https://doi.org/10.1021/jp805657t>
 59. Taleghani, H.G., Ghoreyshi, A.A. and Najafpour, G., "Lactic acid production with in situ extraction in membrane bioreactor", *Applied Food Biotechnology*, Vol. 4, No. 1, (2017), 27-34. <https://doi.org/10.22037/afb.v4i1.13686>
 60. Taleghani, H.G., Ghoreyshi, A.A. and Najafpour, G.D., "Thin film composite nanofiltration membrane for lactic acid production in membrane bioreactor", *Biochemical Engineering Journal*, Vol. 132, (2018), 152-160. <https://doi.org/10.1016/j.bej.2018.01.020>
 61. Abdollahzadeh Sharghi, E., Shorgashti, A. and Bonakdarpour, B., "The study of organic removal efficiency and membrane fouling in a submerged membrane bioreactor treating vegetable oil wastewater", *International Journal of Engineering, Transactions C: Aspects*, Vol. 29, No. 12, (2016), 1642-1649. doi: 10.5829/idosi.ije.2016.29.12c.02

COPYRIGHTS

©2023 The author(s). This is an open access article distributed under the terms of the Creative Commons Attribution (CC BY 4.0), which permits unrestricted use, distribution, and reproduction in any medium, as long as the original authors and source are cited. No permission is required from the authors or the publishers.



Persian Abstract

چکیده

در این مطالعه، به منظور بهبود عملکرد غشاهای پل یکریناتی برای تصفیه پساب‌های روغنی، غشاهای ماتریس مخلوط اولترافیلتراسیون جدید توسط نانوپرکننده اکسید گرافن و نانولوله های هالوسیت عامل دار شده، سنتز شدند. مورفولوژی و سایر خواص غشاهای ساخته شده توسط میکروسکوپ الکترونی روبشی انتشار میدانی، طیف‌سنج FTIR، زاویه تماس و دستگاه مقاومت مکانیکی مشخصه یابی شدند. نتایج به‌دست‌آمده تأیید کرده است که افزودن GO/FHNTs تأثیر مثبتی بر آب‌دوستی و استحکام کششی دارد. همچنین فلاکس اب خالص غشای بهینه GO0.25-FHNT0.75 حدود ۲.۵ برابر بیشتر از پلی کربنات خالص بود. نتایج کلی نشان داده است که همه غشاهای در زمان‌های مختلف فرآیند اولترافیلتراسیون، به بازده ۱۰۰ درصد جداسازی روغن از آب رسیدند. علاوه بر این، غشای بهینه نسبت بازایی شار بیش از ۹۰ درصد را نشان داد است. در عملیات بازایی غشا، شار نفوذی محلول‌های خوراکی با غلظت‌های ۱۰۰ ppm و ۲۰۰ ppm روغن زیتون به ترتیب تنها حدود ۵/۵ درصد و ۶ درصد پس از سه چرخه بازسازی کاهش یافته است.